ELSEVIER

Biophysical Chemistry 56 (1995) 23–29

Biophysical Chemistry

High-resolution structural studies of the retinal–Glu113 interaction in rhodopsin

May Han *, Steven O. Smith

Department of Molecular Biophysics and Biochemistry, Yale University, 266 Whitney Ave. Box 208114, New Haven, CT 06520-8114, USA

Abstract

The key to understanding the reaction mechanism of rhodopsin lies in determining the structure of the retinal binding site and in defining the charge interactions between Glu113 and the retinal protonated Schiff base chromophore. We have been using ^{13}C-NMR chemical shift data to determine the location of the Glu113 carboxyl side chain in relation to the retinal. The NMR data constrain one of the carboxylate oxygens of Glu113 to be ca. 3 Å from the C_{12} position of the retinal with the second oxygen oriented away from the conjugated chain. A water molecule forming a hydrogen bond with the Schiff base is incorporated into the model to account for the high C=N stretching frequency [Han et al., Biophys. J., 65 (1993) 899]. In this study, we have refined the counterion position and have shown that it can reproduce the observed chemical shift data as well as the red-shifted absorption maximum of rhodopsin. Furthermore, the retinal binding site geometry derived from the NMR constraints can be readily incorporated into a recent structural model of the apoprotein.

Keywords: Rhodopsin; Solid-state NMR; Molecular orbital calculation; Vision; Retinal

1. Introduction

Rhodopsin is the photoreceptor in vertebrate rod cells responsible for vision at low light intensities [1]. The photoreactive chromophore in the interior of the protein is 11-*cis*-retinal covalently attached to a lysine side chain through a protonated Schiff base (PSB) linkage (Fig. 1). Absorption of a photon initiates a photochemical reaction of the retinal, the first step being rapid *cis* → *trans* isomerization to form the bathorhodopsin intermediate [2]. The light energy absorbed in this process is channeled into the protein, which undergoes a series of conformational changes resulting in the formation of metarhodopsin II. Interaction between metarhodopsin II and the G-protein transducin then initiates a chain of biochemical events leading to the closing of sodium channels in the plasma membrane and hyperpolariza-

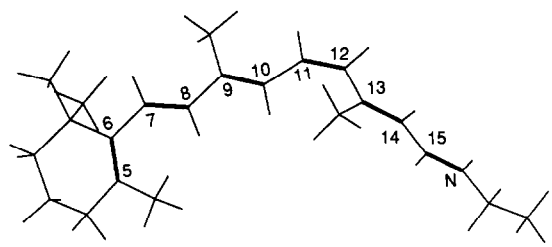

Fig. 1. Structure of the 11-*cis*-retinylidene PSB chromophore.

* Corresponding author.

Elsevier Science B.V.
SSDI 0301-4622(95)00011-9

tion of the rod cell [3]. Several groups using site directed mutagenesis of charged residues in rhodopsin have shown that glutamate 113 serves as the counterion to the positively charged retinal PSB [4–6]. The counterion is likely to be involved in the activation of the rhodopsin protein. Mutation of Glu113 to Gln produces an active form of the protein *in the dark* when regenerated with all-*trans* retinal [5] or simply as the apoprotein [7]. Oprian and coworkers [7,8] have argued that the salt bridge between Glu113 and the retinal PSB is essential for maintaining rhodopsin in the inactive state; breaking this interaction is required for protein activation. Understanding how rhodopsin remains in the inactive state in the dark and how retinal isomerization triggers protein activation requires direct structural data on the charge interactions between Glu113 and the protein-bound retinal PSB.

The retinal chromophore in rhodopsin is a conjugated polyene whose electronic structure is extremely sensitive to surrounding protein charges. Protonation of the retinal-lysine Schiff base linkage adds a net positive charge to the conjugated system that can be localized to the Schiff base proton and two adjacent conjugated carbons, C_{13} and C_{15}, by close association of a negative counterion. Charge delocalization leading to spectral red-shifts may result from simply increasing the separation between the PSB and its associated counterion [9] or from placing charged or polar residues along the conjugated chain that stabilize partial positive charge on the retinal carbons away from the PSB [10,11]. The ^{13}C-NMR chemical shift is sensitive to the electron density surrounding the carbon nucleus, and provides a probe of the partial charge on each carbon of the conjugated retinal chain. We have been studying the structure of the retinal binding site of both rhodopsin and its photointermediates using ^{13}C-magic angle spinning NMR [12–14]. We have been able to determine the position and orientation of the Glu113 counterion relative to the retinal PSB in rhodopsin using the constraints derived from the chemical shifts of the conjugated carbons [15]. The advantage of NMR over vibrational and absorption measurements is that the observed chemical shifts reflect the *local* charge density at each conjugated carbon as well as provide *global* information when the electron density profile along the retinal chain is considered. One clear result thus far is that the counterion does not interact directly with the atoms forming the PSB linkage, but rather is positioned near C_{12} in the middle of the chain. The 'salt bridge' between Glu113 and the Schiff base is indirect, mediated through the conjugated π system and a water molecule.

In this paper, we further refine the relative location of the counterion in the retinal binding site of rhodopsin. As independent support for the model proposed, we have carried out excited state calculations and found that the λ_{max} predicted for the retinal-counterion geometry is also consistent with the experimental data. Finally, the NMR constraints are used to position the retinal chromophore in the interior of a structural model of the rhodopsin apoprotein recently proposed by Baldwin on the basis of sequence analysis of G-protein coupled receptors [16].

2. Methods

Semiempirical methods have been used extensively to calculate electron densities in conjugated systems. A linear relationship between chemical shift and electron density has been observed by several groups with a correlation of ca. 160 ppm per unit charge [17–19]. These studies suggest that the observed chemical shifts can be predicted quantitatively by electronic calculations. In practice, the charge density and chemical shift *differences* between two closely related compounds are considered, rather than their absolute values, as they yield better correlation [15,20]. Excellent correlations are obtained among retinal model compounds using this approach, indicating that the chromophore binding site of retinal proteins can be modeled, as has been shown for bacteriorhodopsin and rhodopsin [15,20].

The ground- and excited-state calculations were performed using the program ZINDO (Zerner, Florida State University). The charge density values were derived using the ZDO (zero differential overlap) basis set, and 11-*cis*-N-retinylidene-n-propyliminium chloride (11-*cis*-RPSB · Cl) was used as a reference state for obtaining the chemical shift and charge density differences. The geometry of the 11-*cis* retinal PSB was obtained as described previously [15].

Table 1
Comparison of the calculated and experimental absorption maxima for all-*trans* retinal model compounds and rhodopsin

Compound	λ_{max} (experimental) nm	λ_{max} (calculated) nm
All-*trans*-RPSB·Cl	442 [a]	447
All-*trans*-RPSB·Br	451 [a]	457
Rhodopsin	500	503

[a] Data from Ref. [9] taken in CCl_4.

The absorption maxima are derived from the $S_0 \rightarrow S_1$ transition energies using configuration interaction (CI); 80 single and 130 double lowest-energy excitations were used in the CI Hamiltonian, corresponding to energy cutoffs of 10 and 12.5 eV, respectively. Calculations of the λ_{max} for several retinal model compounds were used to test the accuracy of the approach. The calculated and experimental results are presented in Table 1.

3. Retinal binding site structure in rhodopsin

We have previously localized the position of the carboxylate counterion to the retinal PSB by analyzing the ^{13}C chemical shifts of the conjugated retinal carbons [15]. In order to fit the chemical shift data, it was necessary to place one of the oxygen atoms (O_1) of the Glu113 carboxylate close to position C_{12} of the retinal, while orienting the second oxygen (O_2) away from the retinal chain. Further refinement of this model has been undertaken in this study in order to restrict the $O_1 \cdots C_{12} \cdots H$ angle θ. This is done by moving a point charge (q^-), representing O_1, around C_{12} in 15° increments from $-135°$ to 135° while maintaining the distance between q^- and C_{12} at 3.0 Å. The linear $q^- \cdots H \cdots C_{12}$ geometry is defined as 0°, and the $H \cdots C_{12} \cdots q^-$ geometry as 180°. The $\pm 135°$ limits are chosen to avoid van der Waals contact between the charge and the C_{13}-methyl group. In each case, the plane defined by the $q^- \cdots C_{12} \cdots H$ atoms is perpendicular to the $C_{11} = C_{12}-C_{13}$ plane unless otherwise indicated. The use of a point charge, instead of a more complex carboxylate group, is used to simplify the calculations and roughly map out the acceptable range for the angle θ. The point charge mimics the O_1 oxygen of the Glu113 carboxyl group in most respects, although it exaggerates the charge delocalization and lowers the slope of the linear correlation.

The linear correlation between the charge density derived from each geometry and the experimental chemical shift data (both referenced to the 11-*cis*-RPSB · Cl^- model compound) is evaluated in Fig. 2. The three parameters that describe the calculated fit to the experimental data (the correlation coefficient, slope and intercept) are plotted as functions of the $q^- \cdots C_{12} \cdots H$ angle θ (Fig. 2a–c). The λ_{max} for each counterion geometry is also calculated and plotted as a function of the angle θ (Fig. 2d). An acceptable fit in this study has a correlation coefficient > 0.80, a slope > 90 ppm/unit charge and an intercept < 1.0 ppm. These limits provide a loose set of constraints and when applied, the resulting acceptable range of θ lies between $-45°$ to 90°. A 60° geometry is chosen for the $O_1 \cdots C_{12} \cdots H$ angle θ of the final proposed structure because it gives one of the best fits to the chemical shift data and also yields the lowest λ_{max} (Fig. 2d) which is necessary to fit the 500 nm rhodopsin absorption when a carboxylate counterion is used later to replace the point charge q^-. Other geometries, however, are not strictly ruled out.

Fig. 3a presents the current model for the retinal binding site having a carboxylate group with O_1 3.0 Å from C_{12}, an $O_1 \cdots C_{12} \cdots H$ angle of 60°, and O_2 oriented away from the retinal chain. A water molecule is incorporated into the proposed structure with its oxygen hydrogen-bonded to the Schiff base and one O–H forming a weak hydrogen bond with O_2 of the carboxylate group as described previously [15]. Fig. 3b illustrates that the charge densities obtained from the structure shown in Fig. 3a nicely reproduce the experimental data derived from the chemical shifts using the 160 ppm/unit charge correlation. The linear correlation between the calculated charge density difference of the model and the experimental chemical shift difference measured in rhodopsin (both referenced to 11-*cis*-RPSB · Cl) yields a correlation coefficient of 0.91, a slope of 172 ppm/unit charge and an intercept of 0.29 ppm (Fig. 3c). Notice that the slope is higher, and also closer to the experimental value (160 ppm/unit charge), when the CH_3-COO^- and H_2O are used to replace the point charge counterion which had yielded

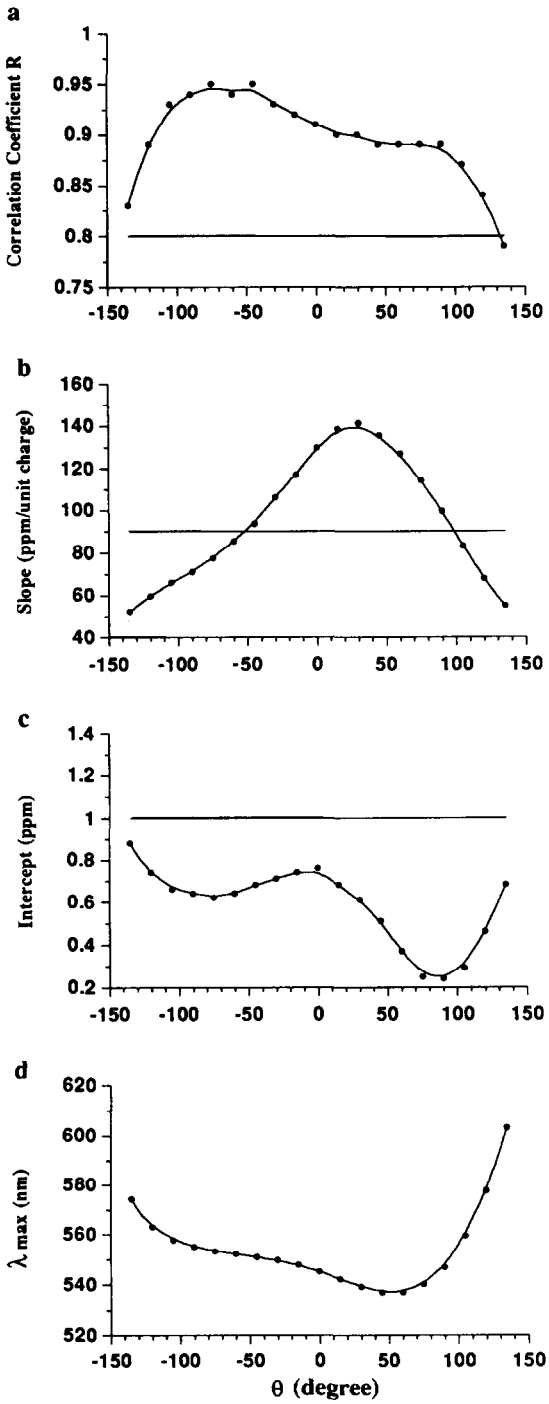

a slope of 127 ppm/unit charge at $\theta = 60°$ (Fig. 2b). The λ_{max} calculated for the model shown in Fig. 3 is 503 nm (Table 1), in excellent agreement with the experimental λ_{max}. The blue shift of the absorption maximum when compared to that calculated with the full point charge at C_{12} (Fig. 2d) is mainly due to the presence of water at the Schiff base. It is necessary to point out that even though the Glu113 counterion and the H_2O are the major determinants for the charge distribution and λ_{max} of the retinal chromophore inside rhodopsin, contributions from other protein groups, especially dipoles of polar residues cannot be ruled out. It has been shown that the presence of hydroxyl groups can account for most, if not all, of the difference in λ_{max} between red and green cone pigments of mammals [21,22]. We have not incorporated dipoles other than the H_2O molecule in the calculation due to the lack of structural data.

A key functional property of the retinal when bound to rhodopsin is the extremely high pK_a of the protonated Schiff base, which is estimated to be > 16 [23]. The high pK_a ensures that the Schiff base is protonated at physiological pH, keeping the λ_{max} of the pigment in the visible range. Maintaining the salt bridge between the retinal PSB and Glu113 contributes to locking the protein in an inactive state [8]. Gat and Sheves argued, on the basis of an elegant set of retinal model compounds, that the pK_a can be increased by specific orientations of the Schiff base and carboxylate counterion that allow structural water molecules to bridge these groups [24]. Recent evidence for water bound near the SB in rhodopsin comes from the observation of rapid hydrogen/deuterium exchange of the Schiff base proton [25]. These data support earlier suggestions that water

Fig. 2. Refinement of the retinal–protein charge interactions in rhodopsin. Charge densities have been calculated for retinal binding site models having a single point charge at 3.0 Å from C_{12} and varying the $q^- \cdots C_{12} \cdots H$ angle (θ) from 135° to −135°. The linear correlation between the charge density derived from each geometry and the experimental chemical shift data (both referenced to 11-*cis*-RPSB·Cl) is evaluated by plotting the correlation coefficient R (a), the slope (b) and the intercept (c) as a function of θ. The cutoffs for an acceptable fit ($R > 0.8$, slope > 90 ppm/unit charge, intercept > 0.0 ppm) are shown as straight lines in each panel. (d) Calculated absorption maxima for each counterion geometry as a function θ.

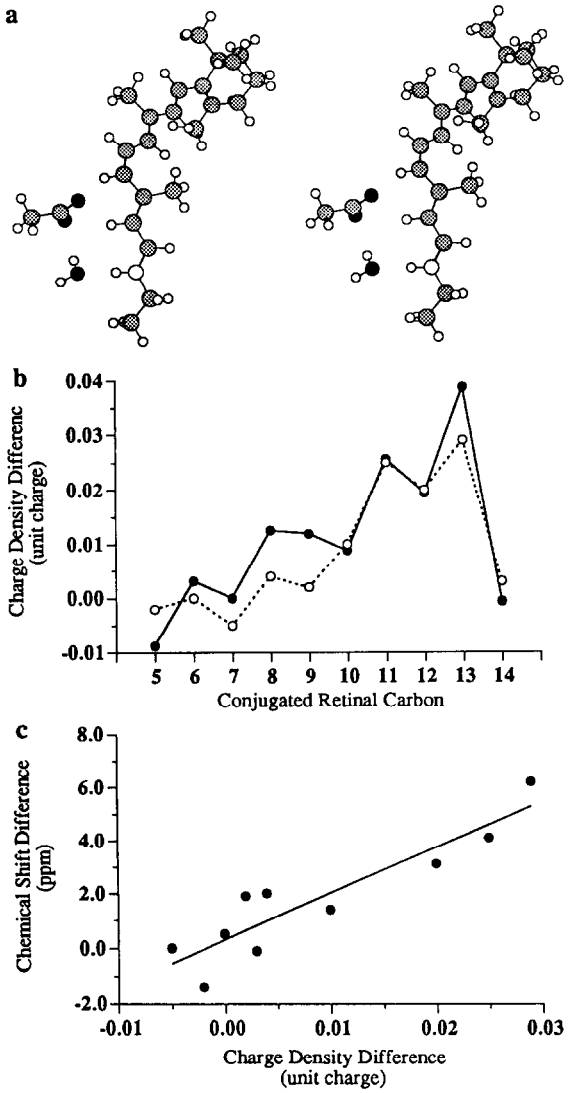

Fig. 3. Modeling the retinal–Glu113 interactions in rhodopsin. (a) Stereo view of the structural model of the retinal binding site with a CH_3–COO^- counterion and H_2O. The key distances are $C_{12} \cdots O_1$ (CH_3–COO^-) 3.0 Å, $C_{12} \cdots O_2$ (CH_3–COO^-) 5.1 Å, N · · · O (water) 2.9 Å, N · · · O_1 4.7 Å and the $O_1 \cdots C_{12} \cdots H$ angle is 60°. (b) Comparison of the charge density differences of the experimental data (●) with a model having a CH_3–COO^- counterion at C_{12} and H_2O at the Schiff base (○). (c) Plot of the linear correlation between the calculated charge density difference of the model and experimental chemical shift difference of rhodopsin. The correlation coefficient is 0.91, the slope is 172 ppm/unit charge and the intercept is 0.29 ppm.

exists in the retinal binding site of rhodopsin [26–28]. The NMR data constrain the carboxylate counterion to be located near the middle of the retinal chain, closest to C_{12}, rather than directly associated with the PSB (Fig. 3a). A water molecule hydrogen bonded to the PSB is incorporated into the model to account for the high C=N frequency and ND shift [29–31]; a weaker hydrogen bond can also be established between the carboxylate and H_2O. Together, these results indicate that the salt bridge between Glu113 and the retinal is, at least in part, mediated by water.

4. Positioning the retinal chromophore in rhodopsin

In the past year, Henderson and coworkers have obtained a 9 Å projection map of rhodopsin [32]. In parallel with these studies, Baldwin has modeled the location, rotational orientation and tilt of the seven transmembrane helics based on a sequence analysis of 204 G-protein coupled receptors, including rhodopsin [16]. The arrangement of the helices in this model agrees well with the projection map. Support for both the helix assignments and rotational orientations of helices II, III and VII comes from a G90D mutation that constitutively activates rhodopsin. Oprian and coworkers [33] found that Asp 90 in mutants G90D or G90D/E113A can either compete with or replace Glu113 as the Schiff base counterion. The double mutant G90D/E113Q, where Asp 90 is the only counterion, has an absorption maximum at 472 nm, blue-shifted compared to wild-type rhodopsin (500 nm) and E113D (510 nm) [34]. This implies that the Schiff base is closer to residue 90 than 113 in rhodopsin.

The Baldwin model of the rhodopsin apoprotein is presented in Fig. 4 where the key amino acid residues have been marked and the Lys 296 and Glu113 side chains are shown in extended conformations. We can readily incorporate the 11-*cis*-retinal chromophore into the seven-helix bundle to accommodate the Glu113 · · · retinal C_{12} interaction derived from the NMR constraints (Fig. 4). Fluorescence energy transfer [35] and linear dichroism [36] measurements indicate that the retinal is located in the center of the lipid bilayer with its transition dipole oriented at an

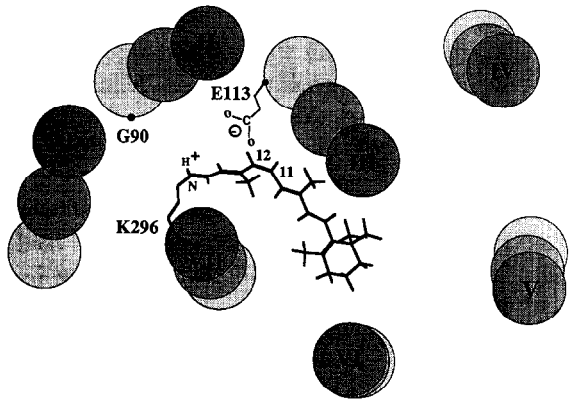

Fig. 4. Model of the retinal binding site in rhodopsin. The seven transmembrane helices are depicted as overlapping circles and are oriented on the basis of the model developed by Baldwin [16]. The lightest circles lie on the intradiscal side of the protein and the darkest circles lie on the cytoplasmic side of the protein. The three residues of interest, Gly 90, Glu 113 and Lys 296, lie close to each other in space. The 11-*cis*-retinal chromophore has been incorporated into the model using the NMR constraints which require a close interaction between Glu 113 and C_{12} of the chromophore.

angle of ca. 16° with respect to the membrane plane. It is necessary to place the retinal plane roughly perpendicular to the helix axis in order to account for these observations and to reproduce the geometry shown in Fig. 2a. The position of the Schiff base in Fig. 4 is also consistent with the idea that it is closer to residue 90 than 113 as indicated by the mutagenesis data discussed above.

The NMR data provide high resolution constraints for establishing the position of Glu113 relative to the retinal chromophore. This enables the retinal to be uniquely docked inside the apoprotein when combined with the other observations described above. The resulting structure (Fig. 4) can serve as a starting point for identifying other residues in the retinal binding site, as well as for modeling the isomerization process in the context of the protein.

Acknowledgment

We thank Dr. J. Baldwin for providing the diagrams of the arrangement of the seven helices at three levels within the membrane. This work was supported by a grant from the National Institutes of Health (GM 41412).

References

[1] J. Nathans, Biochemistry, 31 (1992) 4923.
[2] T. Yoshizawa and G. Wald, Nature, 197 (1963) 1279.
[3] L. Stryer, J. Biol. Chem, 266 (1991) 10711.
[4] E.A. Zhukovsky and D.D. Oprian, Science, 246 (1989) 928.
[5] T.P. Sakmar, R.R. Franke and H.G. Khorana, PNAS, 86 (1989) 8309.
[6] J. Nathans, Biochemistry, 29 (1990) 9746.
[7] P.R. Robinson, G.B. Cohen, E.A. Zhukovsky and D.D. Oprian, Neuron, 9 (1992) 719.
[8] G.B. Cohen, D.D. Oprian and P.R. Robinson, Biochemistry, 31 (1992) 12592.
[9] P.E. Blatz, J.H. Mohler and H.V. Navangul, Biochemistry, 11 (1972) 848.
[10] B. Honig, A.D. Greenberg, U. Dinur and T.G. Ebrey, Biochemistry, 15 (1976) 4593.
[11] A. Kropf and R.T. Hubbard, Ann. NY, Acad. Sci, 74 (1958) 266.
[12] S.O. Smith, I. Palings, M.E. Miley, J. Courtin, H. de Groot, J. Lugtenburg, R.A. Mathies and R.G. Griffin, Biochemistry, 29 (1990) 8158.
[13] S.O. Smith, J. Courtin, H. de Groot, R. Gebhard and J. Lugtenburg, Biochemistry, 30 (1991) 7409.
[14] S.O. Smith, H. de Groot, R. Gebhard and J. Lugtenburg, Photochem. Photobiol, 56 (1992) 1035.
[15] M. Han, B.S. DeDecker and S.O. Smith, Biophys. J, 65 (1993) 899.
[16] J.M. Baldwin, EMBO J, 12 (1993) 1693.
[17] H. Spiesecke and W.G. Schneider, Tetrahedron Lett, 14 (1961) 468.
[18] P.C. Lauterbur, J. Am. Chem. Soc, 83 (1961) 1838.
[19] T. Tokuhiro and G. Fraenkel, J. Am. Chem. Soc, 91 (1969) 5005.
[20] H. Rodman-Gilson and B.H. Honig, J. Am. Chem. Soc, 110 (1988) 1943.
[21] M. Neitz, J. Neitz and Jacobs, Science, 252 (1991) 971.
[22] S. Merbs and J. Nathans Photochem. Photobiol., 58 (1993) 706.
[23] G. Steinberg, M. Ottolenghi and M. Sheves, Biophys. J, 64 (1993) 1499.
[24] Y. Gat and M. Sheves, J. Am. Chem. Soc., 115 (1993) 3772.
[25] H. Deng, L. Huang, R. Callender and T. Ebrey, Biophys. J., 66 (1994) 1129.
[26] C.N. Rafferty and H. Shichi, Photochem. Photobiol., 33 (1981) 229.
[27] D. Cossette and D. Vocelle, Can. J. Chem., 65 (1987) 1576.
[28] J.R. Tallent, E.W. Hyde, L.A. Findsen, G.C. Fox and R.R. Birge, J. Am. Chem. Soc., 114 (1992) 1581.
[29] R. Mathies, T.B. Freedman and L. Styer, J. Mol. Biol, 109 (1977) 367.

[30] T. Bassov, N. Friedman and M. Sheves, Biochemistry, 26 (1987) 3210.
[31] H.S. Rodman-Gilson, B.H. Honig, A. Croteau, G. Zarrilli and K. Nakanishi, Biophys. J., 53 (1988) 261.
[32] G.F. Schertler, C. Villa and R. Henderson, Nature, 362 (1993) 770.
[33] V.R. Rao, G.B. Cohen and D.D. Oprian, Nature, 367 (1994) 639.
[34] T.P. Sakmar, R.R. Franke and H.G. Khorana, PNAS, 88 (1991) 3079.
[35] D.D. Thomas and L. Stryer, J. Mol. Biol, 154 (1982) 145.
[36] P.A. Liebman, Biophys. J, 2 (1962) 161.